J. Mt. Sci. (2017) 14(12): 2620-2630 e-mail: jms@imde.ac.cn http://jms.imde.ac.cn
https://doi.org/10.1007/s11629-017-4364-5

Propagation characteristics of vibration waves induced in surrounding rock by tunneling blasting

CHEN Shi-hai[1,2*] http://orcid.org/0000-0003-4445-3725; e-mail: cshblast@163.com

HU Shuai-wei[1] http://orcid.org/0000-0002-2270-5189; e-mail: 1011483827@qq.com

ZHANG Zi-hua[1] http://orcid.org/0000-0002-7329-0788; e-mail: tsgzhang@163.com

WU Jian[1] http://orcid.org/0000-0002-3074-5543; e-mail: 1032985153@qq.com

* *Corresponding author*

1 Huaqiao University, Xiamen 361021, China

2 Fujian Research Center for Tunneling and Urban Underground Space Engineering, Huaqiao University, Xiamen 361021, China

Citation: Chen SH, Hu SW, Zhang ZH, et al. (2017) Propagation characteristics of vibration waves induced in surrounding rock by tunneling blasting. Journal of Mountain Science 14(12). https://doi.org/10.1007/s11629-017-4364-5

Abstract: The effect of blasting vibration waves on surrounding rock and supporting structures is an important field in underground engineering. In this paper, the separation variable method is used to solve the displacement potential function for the propagation of the blasting vibration waves. In the axis coordinate system, the particle motion and stress change with axial distance, radial distance and time is obtained in surrounding rock. The peak particle velocity law in surrounding rock under different blast loads and surrounding rock parameters is discussed. In addition, the particle vibration characteristics in the surrounding rock are studied using numerical simulations method. The results shows that the peak particle velocity in surrounding rock appears negative exponent attenuation with the increase of axial distance, but it appears positive and negative fluctuations in radial direction. This phenomenon is a new discovery and it has been rarely investigated before. Moreover, the peak particle velocity attenuates more quickly and intensely in the near blasting field, which means that the supporting structure in a shorter distance away from the heading face is vulnerable to the impact of blasting vibration. The attenuation of blasting vibration velocity is closely related to charge length, blasting load amplitude, attenuation index and rock elastic modulus. The numerical simulation accomplishes the same results and then demonstrates the validity of theoretical results.

Received: 12 January 2017
Revised: 14 June 2017
Accepted: 11 September 2017

Keywords: Tunneling blasting; Blasting vibration wave; Surrounding rock; Wave equation; Vibration velocity

Introduction

Blasting vibration is one of the serious hazards associated with underground drilling and blasting. The vibration wave induced by tunneling blasting has different effects on the underground structures. They might induce failures in supporting structures and even cause dynamic rock bursting events in mining. Therefore, an in-depth understanding of the vibration effects induced by tunneling blasting in surrounding rock and supporting structures is critical to the security of underground construction. It is also an important issue in the geotechnical field. Previous researches have shown that variations of displacement and stress over time induced by tunneling blasting in the surrounding rock are difficult to measure in three dimensions. Lamb (1904) developed a stress solution in a semi-infinite space of continuous rock mass. Lv and Zhang (2007) conducted a mechanical analysis of different underground tunnel shapes using the complex variable method. Considering the elastoplasticity of surrounding rock and linings, using a three-dimensional dynamic analysis method, Liu and Wang (2004) investigated the dynamic responses of a tunnel under blasting load. Many researchers studied the dynamic stability of surrounding rock by mainly using numerical simulation to analyze peak particle velocity of the tunnel wall surface. Zuo et al. (2011) analyzed the dynamic damage of tunnel surrounding rock by simulating a circular tunnel under blasting excavation and then discussed the blast-induced particle vibration attenuation characteristics and distribution law of the rock damage. Ma et al. (1998) simulated the propagation of blasting stress waves during underground excavation using AUTODYNA. Shiro and Fung (1979) calculated vibration of surrounding rock when exposed to a vibration source in underground tunnels using dynamic finite element method. Li et al. (2011) simulated the propagation process of seismic waves in the elastoplastic tunnel rock under initial stress, and analyzed the propagation and attenuation laws of seismic waves around tunnel based on ANSYS/LS-DYNA simulation. The results indicated that the amplitude attenuated by negative exponential law in the coal and rock, and the acceleration amplitude of seismic wave decayed rapidly in near field and slowly in far field. These research results could not reveal the mechanism of the propagation of blasting vibration wave in surrounding rock in detail.

For the existing tunnels, the dynamic stability of shotcrete is equally important, Ahmed and Ansell (2014) used a finite element method to analyze the behavior of shotcrete and describe the propagation of the stress wave in two dimensions during tunneling blasting operation, and the given recommendations emphasized that blasting should be avoided in the first 12h after shotcreting. Sun et al. (2011) investigated the stability of jointed rock caused by blasting excavation in underground tunnels using the dynamic numerical simulation of the discrete element method and found that rock mass joints loose when normal stress unloads transiently.

Because of the popularization of numerical simulation and testing technique, field test and numerical simulation are commonly used in blasting operation. Cai and Kaiser (2005) presented a numerical analysis with field monitoring data from a granite tunnel to demonstrate how micro-seismicity could be quantitatively linked to the dynamic properties of the rock mass. Yilmaz and Unlu (2014) investigated the applicability of the modified Holmberg-Persson approach in modeling the site specific attenuation of blast waves in rock mass for a tunnel blast design. Osinov (2011) discussed the numerical modeling of a wave in saturated granular soil around a cylindrical tunnel with a tube-type lining.

Besides, many studies of blast-induced vibration effects were concentrated on adjacent tunnels and ground vibration, not on tunnel itself. Shi et al. (2008) analyzed the vibration effect of surrounding rock using the FLAC^{3D} numerical program in a small neighborhood tunnel blasting excavation. Shin et al. (2011) used a numerical method to identify the effects of blast-induced vibration on immediately adjacent tunnel in soft rock. Jetschny et al. (2010) used 3D seismic finite difference modeling and analytical solution of the wave equation in cylindrical coordinate to study the propagation characteristics of tunnel surface-waves, and to ensure the safety and efficiency of tunnel construction.

In conclusion, because of the complexity of tunneling blasting, there is no an analytical solution available to discuss the dynamic action associated with the propagation of stress and particle velocity in the surrounding rock of its own tunnel. In this paper, the vibration wave propagation induced in the surrounding rock of its own tunnel is studied by the means of elasticity theory and mathematical physics.

1 Analytical Solution of Blasting Vibration Wave

For the blasting excavation of an underground tunnel, the tunnel section is simplified to be a circle and the full-face millisecond blasting method and cylindrical charge are used. Because only the contour blasting is considered for calculation, the pressure on tunnel working surface is relatively small and the pressure on working surface is neglected. Therefore, only the radial blasting load is considered in this paper. The radial blasting load acting on the tunnel wall surface in each blasting excavation cycle is treated as a vibration source. Here, it is assumed that the blasting load causing the surrounding rock vibration undergoes negative exponential attenuation with time (Chen et al. 2011). The formula of blasting load $p = A_0 e^{-\alpha t'}$ is used and the load curve is shown in Figure 1. Where, p is the blasting load (Pa), A_0 is the amplitude of the blasting load (Pa) and can be obtained through the blasting theory. α is the attenuation index related to the characteristics of explosives, t' is blasting load action time (s). Here, it is expressed as

$$A_0 = \frac{1}{8}\frac{d_b}{s_b}\left(\frac{d_p}{d_b}\right)^{-2.2}\rho_0 D^2 \tag{1}$$

where, ρ_0 is the explosive density (kg/m3), D is the explosive detonation velocity (m/s), d_b is the diameter of the blasting hole (mm), d_p is the crushed diameter (mm). Generally, d_p= 2.5d_b, s_b is the blast hole spacing (mm).

The deep underground blasting excavation in circular tunnel is a spatial axisymmetric problem, which can be shown in a two-dimensional plane (Figure 2). Where, b is the loaded length (or charge length (m)), r and z are the radial and axial coordination.

In the three-dimensional axisymmetric cylindrical coordinates, the displacement potential function Ψ does not vary with the azimuth angle, but it is related to the radial displacement, axial displacement, and time. The wave equation (Yang et al. 1990) is

$$\nabla^2\Psi = \left(\frac{\partial^2}{\partial r^2} + \frac{1}{r}\frac{\partial}{\partial r} + \frac{\partial^2}{\partial z^2}\right)\Psi = \frac{1}{c_p^2}\frac{\partial^2\Psi}{\partial t^2} \tag{2}$$

where, c_p is the longitudinal wave velocity in the surrounding rock, r is the radial distance, z is the axial distance, t is the time.

Separation variable method is used to solve Eq. (2). Taking $\Psi = R(r)Z(z)T(t)$ and abbreviating as $\Psi = RZT$, and substituting it into Eq. (2), the

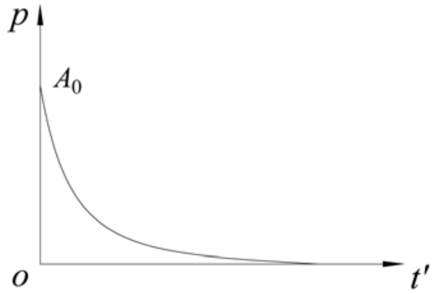

Figure 1 Blasting load curves. p is the blasting load (Pa), A_0 is the amplitude of the blasting load (Pa), t' is blasting load action time (s).

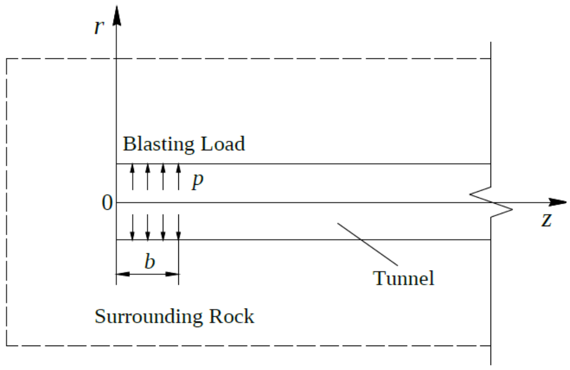

Figure 2 Calculation model of the propagation of the vibration wave induced by blasting in the tunnel.

wave equation can be changed to

$$ZTR'' + \frac{1}{r}R'ZT + RTZ'' = \frac{1}{c_p^2}RZT'' \tag{3}$$

where Z, T and R are the variables associated with the axial distance, time and radial distance, respectively. By dividing both sides of the equation of ZTR and introducing a real constant m, Eq. (3) can be expressed as

$$\frac{R''}{R} + \frac{1}{r}\frac{R'}{R} + \frac{Z''}{Z} = \frac{1}{c_p^2}\frac{T''}{T} = m^2 \tag{4}$$

In order to simplify the calculation, observing the right side of Eq.(4), T can be expressed as

$$T = C_1 e^{mc_p t} + C_2 e^{-mc_p t} \tag{5}$$

where C_1 and C_2 are constants related to the boundary conditions, when $t \to \infty$, the vibration in the surrounding rock is zero, and Eq. (5) becomes

$$T = C_2 e^{-mc_p t} \tag{6}$$

By introducing a real constant, n into right side of Eq. (4), there is

$$\frac{R''}{R} + \frac{1}{r}\frac{R'}{R} - m^2 = -\frac{Z''}{Z} = -n^2 \tag{7}$$

According to the Eq. (7), Z can be obtained as

$$Z = B_1 e^{nz} + B_2 e^{-nz} \quad (8)$$

where B_1 and B_2 are constants. Similarly, $\lim_{z\to\infty} Z = 0$, so

$$Z = B_2 e^{-nz} \quad (9)$$

The left side of Eq. (7) can be converted to a zeroth-order Bessel equation, and the solution can be expressed as (Wang 2011)

$$R = CJ_0\left(\sqrt{n^2 - m^2}\,r\right) \quad (10)$$

When $\sqrt{n^2 - m^2}\,r$ is relatively large, it comes to an approximate relationship

$$R = C\sqrt{\frac{2}{\pi\sqrt{n^2 - m^2}\,r}}\cos(\sqrt{n^2 - m^2}\,r - \frac{\pi}{4}) \quad (11)$$

where C is a constant. Combining Eqs. (6), (9) and (11) together, the displacement potential function can be gotten as

$$\Psi = C\sqrt{\frac{2}{\pi\sqrt{n^2 - m^2}\,r}}\cos(\sqrt{n^2 - m^2}\,r - \frac{\pi}{4})e^{-nz}e^{-mc_p t} \quad (12)$$

According to the relationship between the displacement potential function and the displacement in cylindrical coordinates, the radial displacement U_r, the tangential displacement U_θ, and the axial displacement W, are obtained respectively (Achenbach 1975).

$$U_r = \frac{\partial\Psi}{\partial r} = A_1\left[\frac{1}{2}r^{-\frac{3}{2}}\cos\left(\sqrt{n^2 - m^2}\,r - \frac{\pi}{4}\right) + r^{-\frac{1}{2}}\sqrt{n^2 - m^2}\sin\left(\sqrt{n^2 - m^2}\,r - \frac{\pi}{4}\right)\right]e^{-nz}e^{-mc_p t} \quad (13)$$

$$U_\theta = 0 \quad (14)$$

$$W = \frac{\partial\Psi}{\partial z} = A_2 r^{-\frac{1}{2}}\cos\left(\sqrt{n^2 - m^2}\,r - \frac{\pi}{4}\right)e^{-nz}e^{-mc_p t} \quad (15)$$

where A_1 and A_2 are constants, $A_1 = -C\sqrt{\frac{2}{\pi\sqrt{n^2 - m^2}}}$, $A_2 = -nC\sqrt{\frac{2}{\pi\sqrt{n^2 - m^2}}}$, which means that, $A_2 = n A_1$.

When t=0, r=r_0 and W=0, it can be obtained that $\cos(\sqrt{n^2 - m^2}\,r_0 - \pi/4) = 0$ from Eq. (15).

So, $\sqrt{n^2 - m^2}\,r_0 - \frac{\pi}{4} = k\pi + \frac{\pi}{2}, (k = 0,1,2,3\cdots)$.

Namely, $\sqrt{n^2 - m^2} = \frac{\pi}{r_0}(k + \frac{3}{4}), (k = 0,1,2,3\cdots)$.

In which, k is a nature number (k= 0, 1, 2, 3…), it is on behalf of the multi-value properties of cosine function, r_0 is the radius of the circular tunnel.

In the cylindrical coordinates, the radial velocity, tangential velocity and axial velocity are respectively (Achenbach 1975).

$$V_r = -mc_p A_1\left[\frac{1}{2}r^{-\frac{3}{2}}\cos\left(\sqrt{n^2 - m^2}\,r - \frac{\pi}{4}\right) + r^{-\frac{1}{2}}\sqrt{n^2 - m^2}\sin\left(\sqrt{n^2 - m^2}\,r - \frac{\pi}{4}\right)\right]e^{-nz}e^{-mc_p t} \quad (16)$$

$$V_\theta = 0 \quad (17)$$

$$V_z = -mc_p A_2 r^{-\frac{1}{2}}\cos\left(\sqrt{n^2 - m^2}\,r - \frac{\pi}{4}\right)e^{-nz}e^{-mc_p t} \quad (18)$$

According to the relationship between the stress and displacement in the axisymmetric cylindrical coordinates (Xu 2006; Lu 1990), the stress can be obtained as

$$\sigma_{rr} = \frac{E}{1+\mu}\left(\frac{\mu}{1-2\mu}\Theta + \frac{\partial U_r}{\partial r}\right) \quad (19)$$

$$\sigma_{\theta\theta} = \frac{E}{1+\mu}\left(\frac{\mu}{1-2\mu}\Theta + \frac{U_r}{r}\right) \quad (20)$$

$$\sigma_{zz} = \frac{E}{1+\mu}\left(\frac{\mu}{1-2\mu}\Theta + \frac{\partial W}{\partial z}\right) \quad (21)$$

$$\Theta = \varepsilon_r + \varepsilon_\phi + \varepsilon_z = \frac{\partial U_r}{\partial r} + \frac{U_r}{r} + \frac{\partial W}{\partial z} \quad (22)$$

where σ_{rr}, $\sigma_{\theta\theta}$ and σ_{zz} are the radial stress, tangential stress, and axial stress, respectively, and Θ is the volumetric strain.

Substituting Eqs. (13), (14) and (15) into Eq. (22), the volumetric strain can be obtained as

$$\Theta = -A_1\left[m^2 r^{-\frac{1}{2}}\cos\left(\sqrt{n^2 - m^2}\,r - \frac{\pi}{4}\right) + \frac{1}{4}r^{-\frac{5}{2}}\cos\left(\sqrt{n^2 - m^2}\,r - \frac{\pi}{4}\right)\right]e^{-nz}e^{-mc_p t} \quad (23)$$

Substituting Eqs. (13)-(15) and (23) into Eqs. (19), (20) and (21), the stress can be obtained as

$$\sigma_{rr} = \frac{EA_1}{1+\mu}\left[-\sqrt{n^2 - m^2}\,r^{-\frac{3}{2}}\sin\left(\sqrt{n^2 - m^2}\,r - \frac{\pi}{4}\right) - \frac{3-5\mu}{4(1-2\mu)}r^{-\frac{5}{2}}\cos\left(\sqrt{n^2 - m^2}\,r - \frac{\pi}{4}\right)\right]e^{-nz}e^{-mc_p t} \quad (24)$$

$$\sigma_{\theta\theta} = \frac{EA_1}{1+\mu}\left[\sqrt{n^2-m^2}r^{-\frac{3}{2}}\sin\left(\sqrt{n^2-m^2}r-\frac{\pi}{4}\right)\right.$$
$$-\frac{\mu m^2}{1-2\mu}r^{-\frac{1}{2}}\cos\left(\sqrt{n^2-m^2}r-\frac{\pi}{4}\right)$$
$$\left.+\frac{2-5\mu}{4(1-2\mu)}r^{-\frac{5}{2}}\cos\left(\sqrt{n^2-m^2}r-\frac{\pi}{4}\right)\right]e^{-nz}e^{-mc_pt} \quad (25)$$

$$\sigma_{zz} = \frac{EA_1}{1+\mu}\left[\frac{(2n^2-m^2)\mu-n^2}{1-2\mu}r^{-\frac{1}{2}}\cos\left(\sqrt{n^2-m^2}r-\frac{\pi}{4}\right)\right.$$
$$\left.-\frac{\mu}{4(1-2\mu)}r^{-\frac{5}{2}}\cos\left(\sqrt{n^2-m^2}r-\frac{\pi}{4}\right)\right]e^{-nz}e^{-mc_pt} \quad (26)$$

The load boundary condition in the tunnel blasting excavation is

$$\sigma_{rr}\Big|_{0\le z\le b, r=r_0} = p = A_0 e^{-\alpha t'} \quad (27)$$

where b is loaded length (or charge length (m)).

By substituting Eq. (24) into Eq. (27), it can be obtained that

$$A_1 = \frac{A_0}{A} \text{ and } m = \frac{\alpha}{c_p} \quad (28)$$

where,

$$A = \frac{1-e^{-bn}}{bn}\frac{E}{1+\mu}\left[-\sqrt{n^2-m^2}r_0^{-\frac{3}{2}}\sin\left(\sqrt{n^2-m^2}r_0-\frac{\pi}{4}\right)\right.$$
$$+\frac{n^2-m^2+(2n^2-3m^2)\mu}{1-2\mu}r_0^{-\frac{1}{2}}\cos\left(\sqrt{n^2-m^2}r_0-\frac{\pi}{4}\right)$$
$$\left.-\frac{3-5\mu}{4(1-2\mu)}r_0^{-\frac{5}{2}}\cos\left(\sqrt{n^2-m^2}r_0-\frac{\pi}{4}\right)\right].$$

Thus, the radial and axial stresses in the surrounding rock can be obtained by this way.

2 Analytic and Numerical Calculation

2.1 Analytic calculation of particle vibration velocity

For an underground blasting excavation engineering with the millisecond blasting technique, the charge length is 1.5m. The diameters of the blasting holes are 40 mm, and the hole spacing is 45cm. The radius of the circular tunnel is 2.5 m. An emulsion explosive is used, with a density of 1100 kg/m3, and the detonation velocity of 3200 m/s. The rock material of the tunnel is weathered granite. The rock density is 2350 kg/m3, its elastic modulus is 18 GPa, and its Poisson's ratio is 0.25. The blasting load attenuation index is assumed to be 4000. The main parameters of tunneling blasting are illustrated in Table 1. The material parameters of the surrounding rock are illustrated in Table 2.

Table 1 Main parameters of tunneling blasting

Blast hole diameter (mm)	Crushed zone diameter (mm)	Explosive density (kg/m3)	Detonation velocity (m/s)
40	100	1100	3200
Blast hole spacing (mm)	Attenuation index	Tunnel radial (m)	Charge length (m)
450	4000	2.5	1.5

Table 2 Material parameters of surrounding rock

Rock density (kg/m3)	Elasticity modulus (GPa)	Poisson ratio
2350	18	0.25

In order to study the changing law of particle vibration velocity in the surrounding rock with axial distance and radial distance, the parameters are substituted into Eqs. (16)-(18) and calculated by Matlab program. The results are shown in Figure 3 and Figure 4. Because the particle vibration velocity in the surrounding rock has multiple solutions about k, different values of k will be taken for the calculation. Here, k is the nature number.

Figure 3 indicates that the peak particle velocities in the surrounding rock appear the sign wave attenuation with the increase of radial distance. Figure 4 indicates that the peak particle velocities in the surrounding rock appear negative exponent attenuation with the increase of axial distance. Moreover, the peak particle velocities attenuate more quickly and intensely in the near field, which means that the supporting structure in a shorter distance away from the heading face is vulnerable to the impact of blasting vibration.

According to Figure 3 and Figure 4, when k=1, 2, 3···, the peak particle velocity in the surrounding rock is much smaller than that when k =0. Thus, we can take k =0 for the following calculations.

2.2 Numerical calculation of particle vibration velocity

The numerical simulation is established based on the tunnel model in Figure 2. The constitutive model of the rock is simplified as a linear elastic

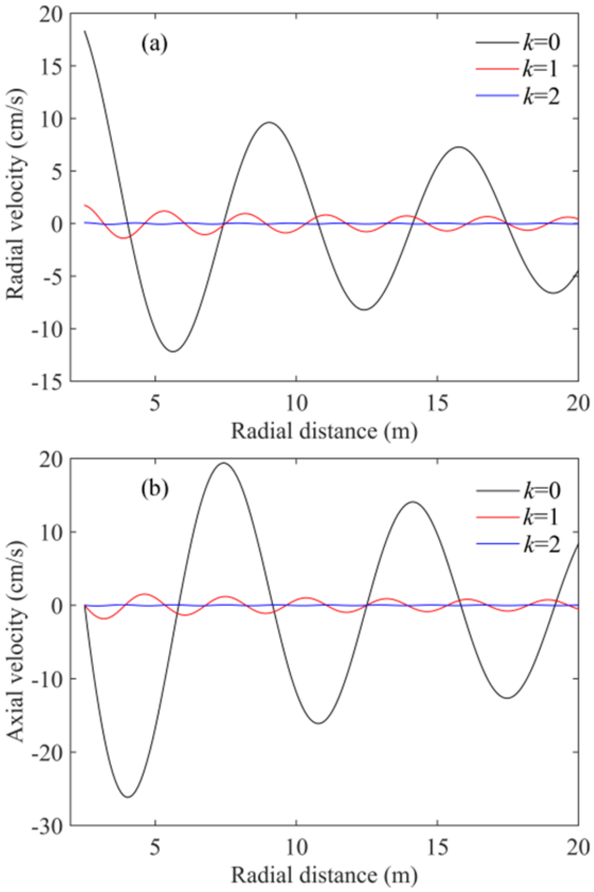

Figure 3 Radial peak particle velocity (a); axial peak particle velocity (b) changes with radial distance in surrounding rock when z=3 m.

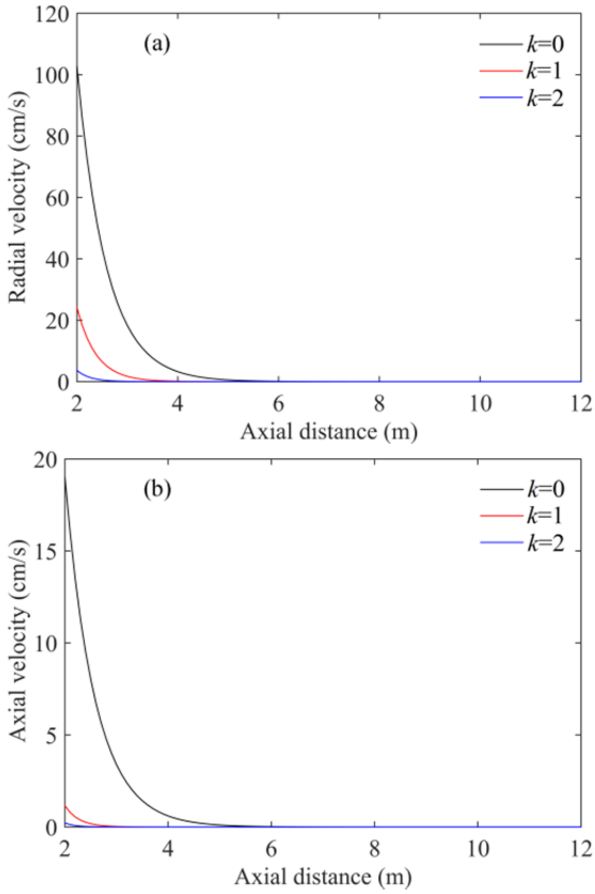

Figure 4 Radial peak particle velocity (when r=2.5m) (a); axial peak particle velocity (when r=6 m) (b) changes with axial distance in surrounding rock.

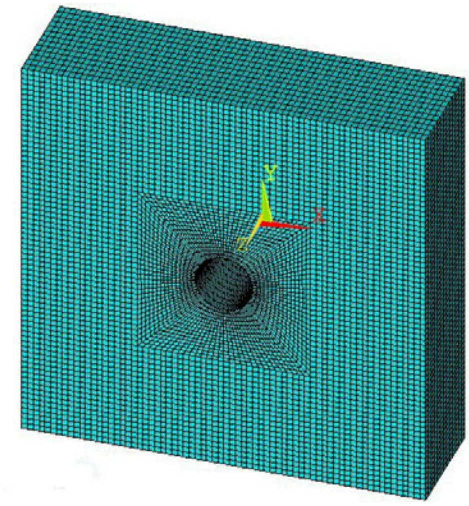

Figure 5 Meshed numerical calculation model.

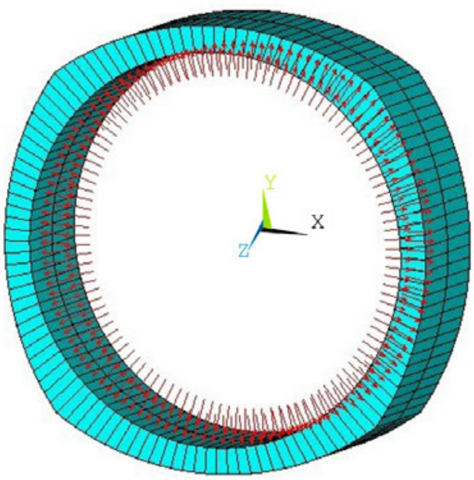

Figure 6 Form of blasting equivalent load on the internal wall of tunnel.

model of continuum material, and a non-reflective boundary condition is used. The size of the model is 35 m × 35 m × 11.5 m. The mesh model includes 84,000 nodes and 75,400 elements and is shown in Figure 5.

A component is proposed in the internal wall of tunnel for the application of equivalent blasting load, and is shown in Figure 6.

The stress and velocity at various points inside the rock are obtained using LS-DYNA. Figure 7 shows the particle velocity contours in the surrounding rock at t = 0.00507 s. The radial velocity propagation of the vibration wave in the rock is manifested as alternating positive and negative, and the velocity decreases nonlinearly with radial distance.

The peak particle velocity in surrounding rock under the blasting load can be obtained through the numerical simulation. Figure 8 shows the change of the simulated peak particle velocity.

Comparing Figure 3a and Figure 8a, it is found that the numerical and analytical results of radial peak particle velocity changing with radial distance are similar, and the maximum value is

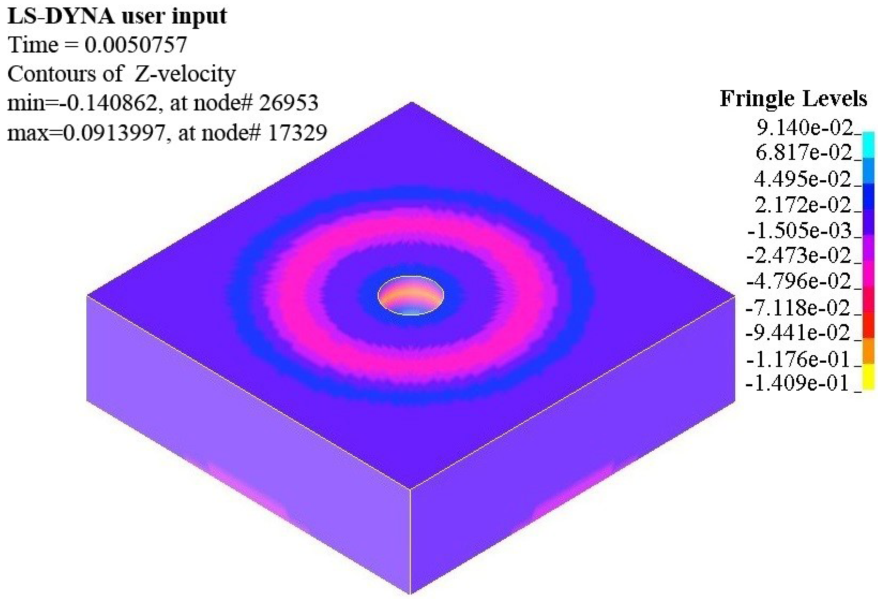

Figure 7 Particle velocity in the surrounding rock at t = 0.00507s.

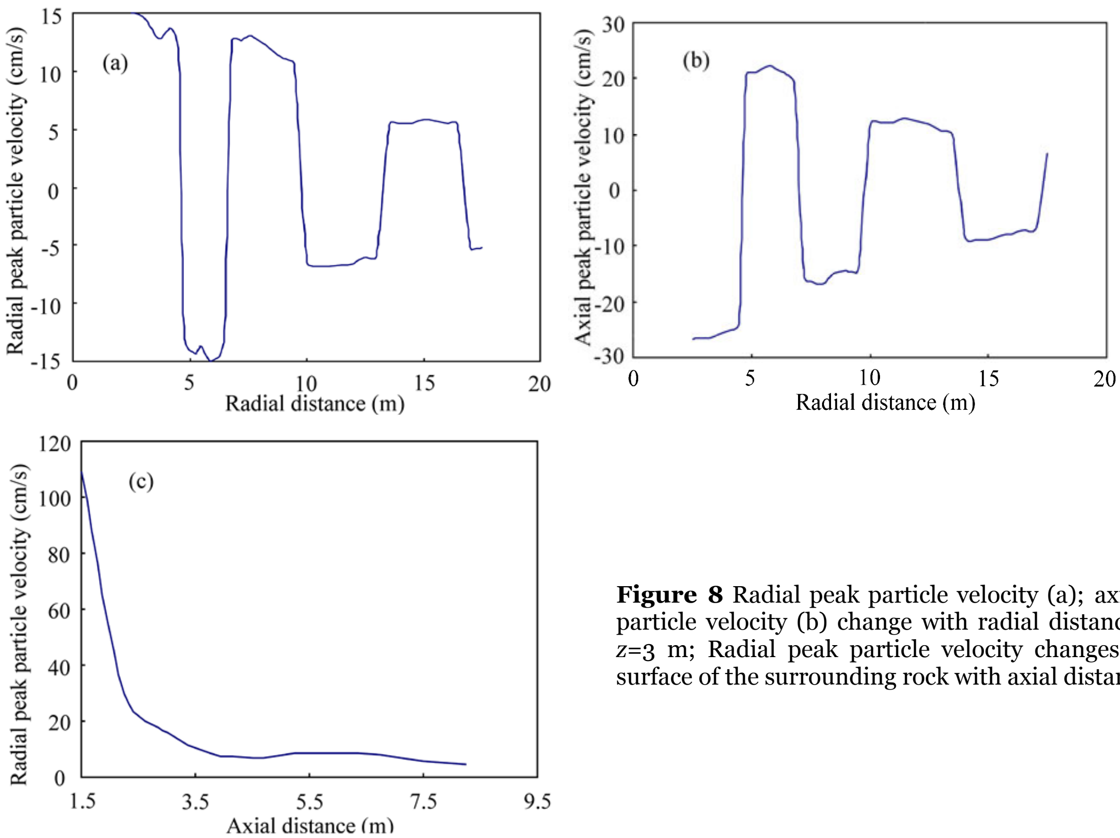

Figure 8 Radial peak particle velocity (a); axial peak particle velocity (b) change with radial distance when z=3 m; Radial peak particle velocity changes on the surface of the surrounding rock with axial distance (c).

approximately 15cm/s. The attenuations with radial distance are in positive and negative alternation forms. Comparing Figure 3b and Figure 8b, the same laws of axial peak particle velocity is obtained, and the maximum value is approximately 25cm/s. While the maximum value of radial peak particle velocity in Figure 4a and Figure 8c is about 100 cm/s, and the attenuation with axial distance is a nonlinear decrease similarly.

As shown above, the simulation and analytical results for the velocity fields in the rock induced by tunneling blasting are consistent in both their values and variation trends.

3 Influence Factor Analysis of Vibration Waves

3.1 Blast load attenuation indexes

In order to study the peak particle velocity law in the surrounding rock under different blast load attenuation indexes, the radial peak particle velocity in z=3m, r=2.5m and the axial peak particle velocity in z=3m, r=6m in the surrounding rock are calculated under different blast load attenuation indexes. The results are showed in Figure 9.

Figure 9 indicates that the radial and axial particle velocity change with time in surrounding rock appear negative exponent attenuation under the same attenuation index. It is observed that the bigger the attenuation index is, the shorter the blasting load time is, the smaller the particle velocity is, and the smaller the blasting effect on the surrounding rock and the supporting structure is.

3.2 Charge lengths

The charge length is one of the most basic parameters in tunneling construction. In order to study the peak particle velocity law in the surrounding rock under different charge lengths, the peak particle velocities in the surrounding rock are calculated under different charge lengths. The results are showed in Figure 10 and Figure 11.

Figure 10 and 11 indicate that the charge length has a significant impact on particle vibration velocity in surrounding rock. Currently, the deeper the blast hole is, the bigger the blast effect is. Therefore, the deep borehole blasting has more significant disturbance on surrounding rock.

3.3 Amplitude of the blasting loads

The blasting load amplitude is one of the most important parameters of blasting load. The peak particle velocities with radial and axial distance in the surrounding rock are calculated under different blasting load amplitudes.

Supposing the amplitude of blasting load is A_0=16.67MPa, and A_0 in Eq.(1) is replaced by 0.5 A_0, 1.0A_0 and 2.0A_0 respectively, the calculation results are showed in Figure 12 and Figure 13.

Figure 12 and 13 indicate that the blasting load amplitude has a significant impact on particle vibration velocity in surrounding rock. Currently, the bigger the amplitude of the blasting load is, the bigger the peak particle velocity in surrounding rock is. If decoupling charge blasting is used, the blasting vibration effect on the surrounding rock and the supporting structure can be reduced effectively.

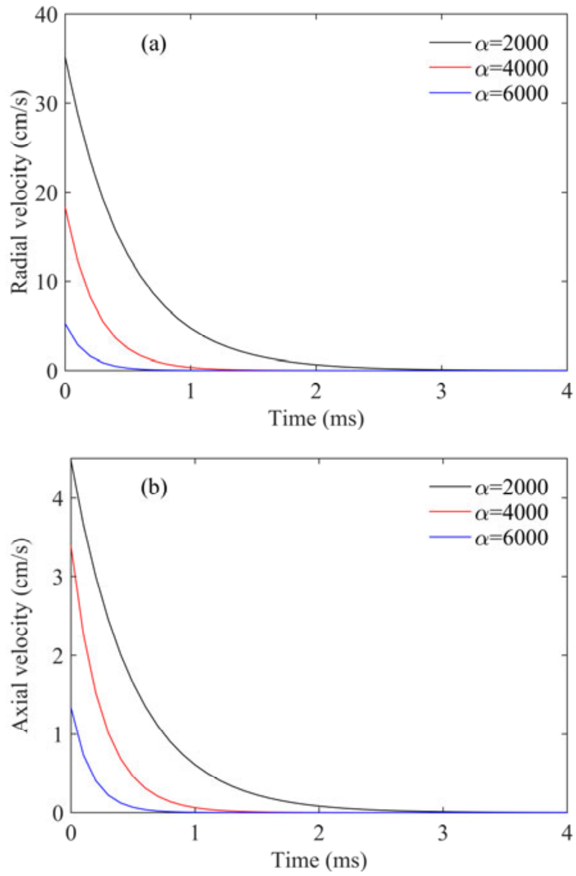

Figure 9 Radial peak particle velocity (a); axial peak particle velocity (b) changes over time in surrounding rock under different attenuation indexes.

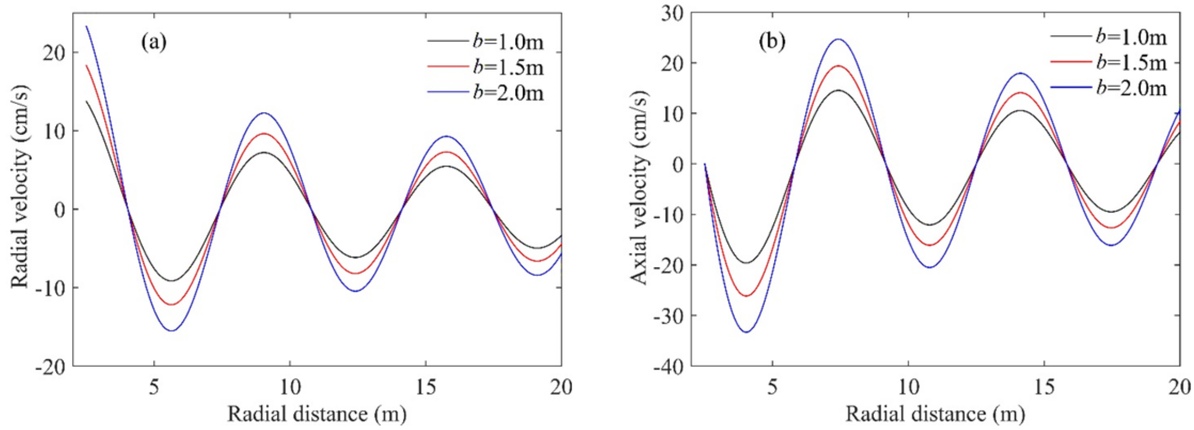

Figure 10 Radial peak particle velocity (a); axial peak particle velocity (b) changes with the radial distance in surrounding rock under different charge lengths when z=3m.

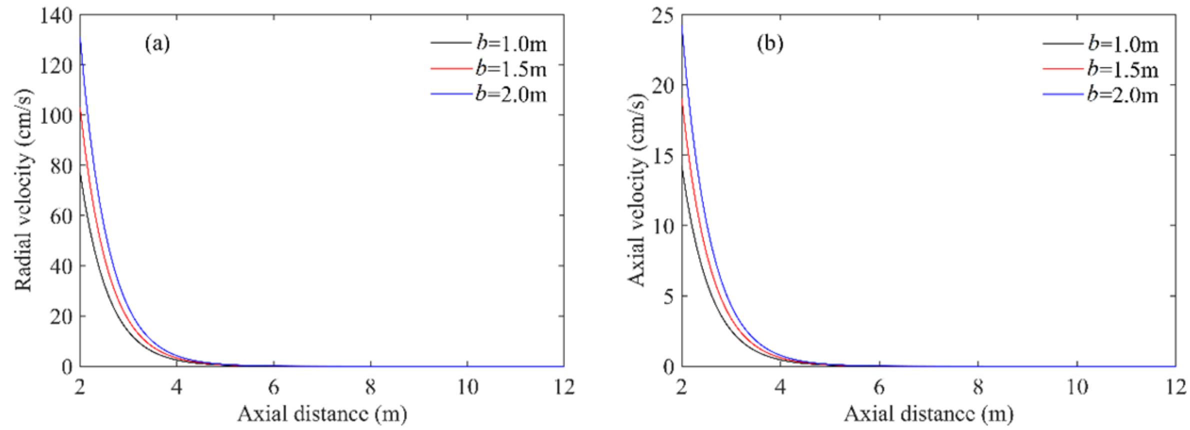

Figure 11 Radial peak particle velocity (when r=2.5 m) (a); axial peak particle velocity (when r=6 m) (b) changes with axial distance in surrounding rock under different charge lengths.

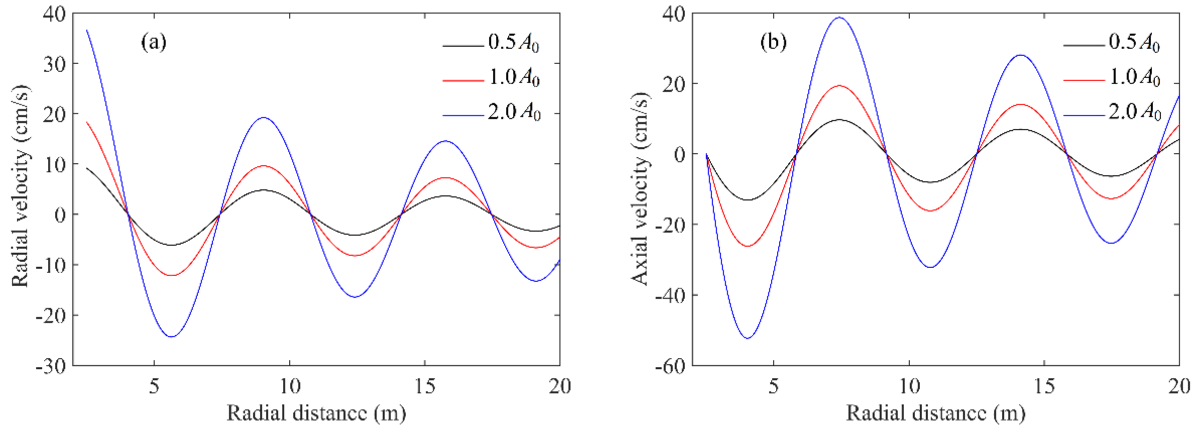

Figure 12 Radial peak particle velocity (a); axial peak particle velocity (b) changes with radial distance in surrounding rock under different amplitudes of the blasting load when z=3 m.

3.4 Rock elastic modulus

In order to study the peak particle velocity law in the surrounding rock under different rock elastic modulus, the radial peak particle velocity in z=3m, r=2.5m and the axial peak particle velocity in z=3m, r=6m are calculated. The calculation result is shown in Figure 14.

Figure 14 indicates that the radial and axial peak particle velocities in the surrounding rock are first increased and then decreased with the increase of the rock elastic modulus. This phenomenon is a new discovery and it's never discussed before.

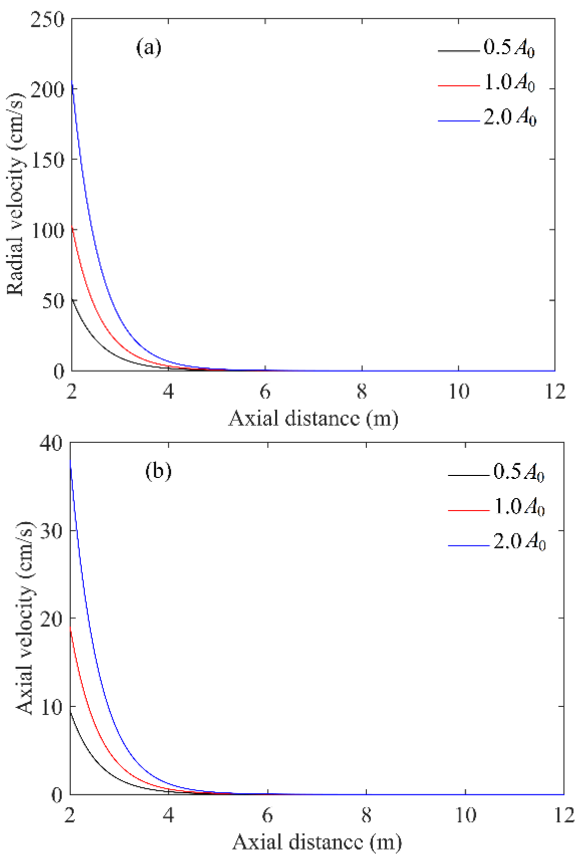

Figure 13 Radial peak particle velocity (a); axial peak particle velocity (b) changes with axial distance in surrounding rock under different amplitudes of the blasting load when r=2.5 m.

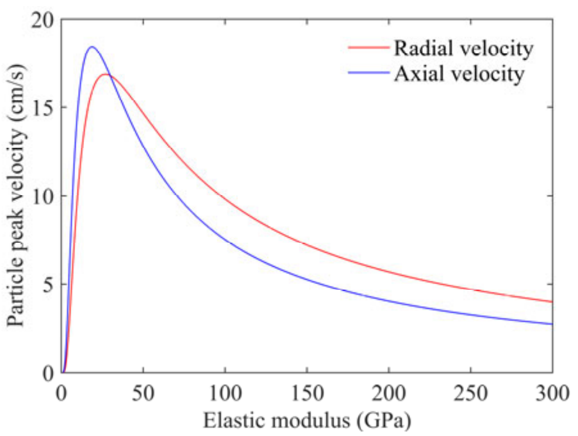

Figure 14 Peak Particle velocity changes with rock elastic modulus.

4 Conclusions

Based on the separation variable method in cylindrical coordinates, the propagation characteristics of blasting vibration wave are investigated by the method of analytic calculation. Furthermore, the factors that affect the blasting vibration waves are discussed. Analytical methods and figures are effective for revealing the mechanisms of the blasting vibration wave propagation. The following conclusions are gotten:

1) The peak particle velocity in surrounding rock appears negative exponent attenuation with the increase of axial distance, but it appears positive and negative fluctuations in radial direction. This phenomenon is a new discovery and it's never discussed before. Moreover, the peak velocity attenuates more quickly and intensely in the near field, which means that the supporting structure in a shorter range away from the heading face is vulnerable to the impact of blasting vibration.

2) The attenuation of blasting vibration velocity is closely related to charge length, blasting load amplitude, attenuation index and rock elastic modulus. Deep borehole blasting has more significant disturbance on surrounding rock. The blasting vibration effect on the surrounding rock and the supporting structure can be reduced effectively by taking decoupling charge blast. It is also observed that the bigger the attenuation index is, the shorter the blasting load time is, the smaller the particle velocity is.

3) The elastic modulus has a significant impact on particle vibration velocity in surrounding rock. The radial and axial peak particle velocity in the surrounding rock are first increased and then decreased with the increase of the rock elastic modulus. This phenomenon is a new research result.

The results help further explain the propagation of blasting vibrations in surrounding rock, and underscore the importance of the proper handling of the relationship between tunneling supports and blasting to ensure their safety during excavations. Besides, this is a preliminary study on the tunnel blasting vibration propagation, and the new research results are found. Deeper research requires a combination with model tests and other means, this is our next work.

Acknowledgments

This work is supported by the National Nature

Science Foundation of China (11672112), the Specialized Research Fund for the Doctoral Program of Higher Education of China (20113718110002), the Fund of the State Key Laboratory of Disaster Prevention & Mitigation of Explosion & Impact (PLA University and Technology) (DPMEIKF201307), Huaqiao University Research Foundation (13BS402).

References

Achenbach JD (1975) Wave Propagation in Elastic Solids. North-Holland Publishing Company, New York, US. pp 121-163.

Ahmed L, Ansell A (2014) Vibration vulnerability of shotcrete on tunnel walls during construction blasting, Tunneling and Underground Space Technology 42(42): 105-111. https://doi.org/10.1016/j.tust.2014.02.008

Cai M, Kaiser PK (2005) Assessment of excavation damaged zone using a micromechanics mode. Tunnelling and Underground Space Technology Incorporating Trenchless Technology Research 20(4): 301-310. https://doi.org/10.1016/j.tust.2004.12.002

Chen SH, Wei HX, Du RQ, et al. (2011) Analysis on Blasting Vibration Effects of Structure. Coal Industry Press, Beijing, China. pp 21-29. (In Chinese)

Jetschny S, Bohlen T, Nil DD (2010) On the propagation characteristics of tunnel surface-waves for seismic prediction. Geophysical Prospecting 58(2): 245-256. https://doi.org/10.1111/j.1365-2478.2009.00823.x

Lamb H (1904) On the propagation of tremors over the surface of an elastic solid. Philosophical Transactions of the Royal Society of London 203: 1-42. https://doi.org/10.1098/ rsta.1904.0013

Li JG, Kang JN, Liu H et al. (2011) Numerical simulation on propagation laws of seismic wave in elastoplastic tunnel rock medium. Journal of China Coal Society 36: 282-286. (In Chinese) https://doi.org/10.13225/j.cnki.jccs.2011.s2.043

Liu GH, Wang ZY (2004) Dynamic response and blast-resistance analysis of a tunnel subjected to blast loading. Journal of Zhejiang University (Engineering Science) 38(2): 204-209. (In Chinese) https://doi.org/10.3785/j.issn.1008-973X.2004.02.017

Lu WM, Luo XF (1990) Basic of Elasticity. Higher Education Press, Beijing, China. pp 147-203. (In Chinese)

Lv AZ, Zhang LQ (2007) Mechanics Analysis with Complex Variables Function in Tunnel Underground. Science Press, Beijing, China. pp 75-110. (In Chinese)

Ma GW, Hao H, Zhou YX (1998) Modeling of wave propagation induced by underground explosion. Computers and Geotechnics 22(3-4): 283-303. https://doi.org/10.1016/S0266-352X(98)00011-1

Osinov VA (2011) Blast-induced wave in soil around a tunnel. Archive of Applied Mechanics 81(5): 543-559. https://doi.org/10.1007/s00419-010-0438-3

Shi HC, Ding N and Zhang JC (2008) Analysis of vibration effects on surrounding rock for small clear distance tunnel under the dynamic action of blasting. Blasting 25(1): 74-78. (In Chinese) https://doi.org/10.3963/j.issn.1001-487X.2008. 01.022

Shin JH, Moon HG, Chae SE (2011) Effect of blast-induced vibration on existing tunnels in soft rocks. Tunneling and Underground Space Technology Incorporating Trenchless Technology Research 26(1): 51-61. https://doi.org/10.1016/j.tust.2010.05.004

Shiro T, Fung N (1979) Surrounding rock vibration analysis methods when the vibration source exist in underground tunnels. Translated by Tan Bingyan. Civil Society Papers Report 28(1): 41-53.

Sun JS, Jin L, Jiang QH, et al. (2011) Loosing mechanism of jointed rock mass induced by transient adjustment of in-situ stress. Journal of Vibration and Shock 30(13): 28-34. (In Chinese) https://doi.org/10.3969/j.issn.1000-3835.2011.12.006

Wang DX (2011) Methods of Mathematical Physics. Science Press, Beijing, China. pp 144-177. (In Chinese)

Xu ZL (2006) Elasticity. Higher Education Press, Beijing, China. pp 73-108. (In Chinese)

Yang BJ, Wang BC, Zhang BJ (1990) Elastic Wave Theory. Northeast Normal University Press, Shenyang, China. pp 178-179. (In Chinese)

Yilmaz O, Unlu T (2014) An application of the modified Holmberg-Persson approach for tunnel blast design. Tunneling and Underground Space Technology 43(6): 113-122. https://doi.org/10.1016/j.tust.2014.04.009

Zuo SY, Xiao M, Xu JK, et al. (2011) Numerical simulation of dynamic damage effect of surrounding rocks for tunnels by blasting excavation. Rock and Soil Mechanics 32(10): 3171-3177. (In Chinese) https://doi.org/10.3969/j.issn.1000-7598.2011.10.046